NASA TECHNICAL NOTE

NASA TN D-3126

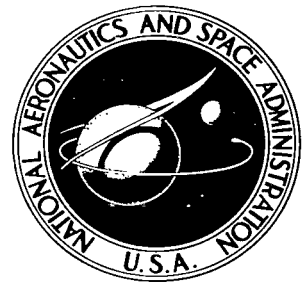

NASA TN D-3126

STRAIN MEASUREMENTS CONDUCTED ON A FULL SCALE ECHO II PASSIVE COMMUNICATIONS SATELLITE BALLOON

by Charles L. Staugaitis and Lawrence Kobren

Goddard Space Flight Center
Greenbelt, Md.

NATIONAL AERONAUTICS AND SPACE ADMINISTRATION • WASHINGTON, D. C. • MARCH 1966

STRAIN MEASUREMENTS CONDUCTED ON A FULL SCALE ECHO II PASSIVE COMMUNICATIONS SATELLITE BALLOON

By Charles L. Staugaitis and Lawrence Kobren

Goddard Space Flight Center
Greenbelt, Md.

NATIONAL AERONAUTICS AND SPACE ADMINISTRATION

For sale by the Clearinghouse for Federal Scientific and Technical Information
Springfield, Virginia 22151 – Price $0.35

ABSTRACT

A photogrammetric method and analysis for determining the strains developed in the skin of the Echo II passive communications satellite in a prelaunch static inflation test is described.

The accuracy of these measurements is questionable due to the complexity of the strain pattern developed, however, a determination of the strain pattern set up in the skin of the "balloon" and reasons for their deviation from a balanced biaxial condition are examined. Comparison of these experimental strain measurements obtained by photogrammetric techniques with values determined from theoretical calculations and reasons for deviations are reviewed.

Finally, tensile properties for the Echo II material obtained from biaxial bulge tests and tensile tests are measured and a comparison of these values with the actual performance of the balloon during the static inflation tests is discussed.

CONTENTS

STRAIN MEASUREMENTS CONDUCTED ON A FULL SCALE ECHO II PASSIVE COMMUNICATIONS SATELLITE BALLOON

by
Charles L. Staugaitis
and
Lawrence Kobren
Goddard Space Flight Center

INTRODUCTION

The first passive communications satellite, Echo I, successfully launched in August 1960, demonstrated the feasibility of deploying a 100 foot diameter inflatable structure in space. The ultimate spherical shape assumed by the *skin* material was maintained by employing a subliming compound whose vapor pressure developed the necessary internal pressure when subjected to a particular temperature environment. The *skin,* consisting essentially of a 0.5 mil film of mylar upon which an aluminum layer was vapor deposited, was sufficiently stretched by the internal pressure to provide the smooth spherical surface necessary for efficient radar reflections. Since the internal pressure remained greater than the ambient, the spherical surface was maintained.

Following this successful event, a new structural concept was inaugurated with the fabrication and subsequent launching on January 25, 1964 of the Echo II passive reflector satellite. In this case, the ultimately high reflecting surface resulted not by the continual presence of an internal gas but from the development of a predetermined amount of plastic deformation in the skin material to produce permanent rigidization after most of the gaseous product had escaped through previously introduced holes. This continued rigidization was possible because the skin material consisted of a metal-polymer laminate having a 0.35 mil mylar film sandwich between two layers of pure aluminum each 0.18 mil thick. Thus, when a predetermined pressure level was reached, the film stretched sufficiently to plastically deform the aluminum layers and yet did not exceed the elastic portion of the stress strain curve of the polymer film. Since the success of the satellite depends primarily on how well it will reflect radar signals while in orbit, its ultimate shape and smoothness become of paramount importance.

To study the structural integrity of a full-sized Echo balloon and to determine the character of the radar response to the composite film envelope at different levels of pressurization, a series of static inflation experiments was conducted at Lakehurst Naval Air Station, Lakehurst, New Jersey, during the months of June, July and December 1963. These full-sized balloon tests were designed to provide information on the degree of envelope spheroidicity, skin texture, structural rigidity, and finally, burst strength of the laminate structure.

The purpose of this paper is to present the results of the photogrammetric strain measurements obtained during the June and December static inflation tests and to assess the effectiveness of this method in determining the extent and distribution of strain developed adjacent to seams, across seams, and within a particular gore. A further objective is to compare the experimental results with theory to ascertain the agreement, if any, that may exist. Finally, an attempt will be made to correlate the strain behavior of a full-scale balloon with data representing laboratory specimens subjected to uniaxial and biaxial stress conditions.

TEST MEASURES AND PROCEDURES

Methods for maintaing balloon stability, programmed inflation rate, and constant lift were devised and successfully implemented at the Lakehurst test site. Briefly, the method used for maintaining a minimum (near neutral) buoyancy depended on obtaining a minimum difference in density between the ambient air and the air within the balloon. Intake and exhaust ports, placed at the top

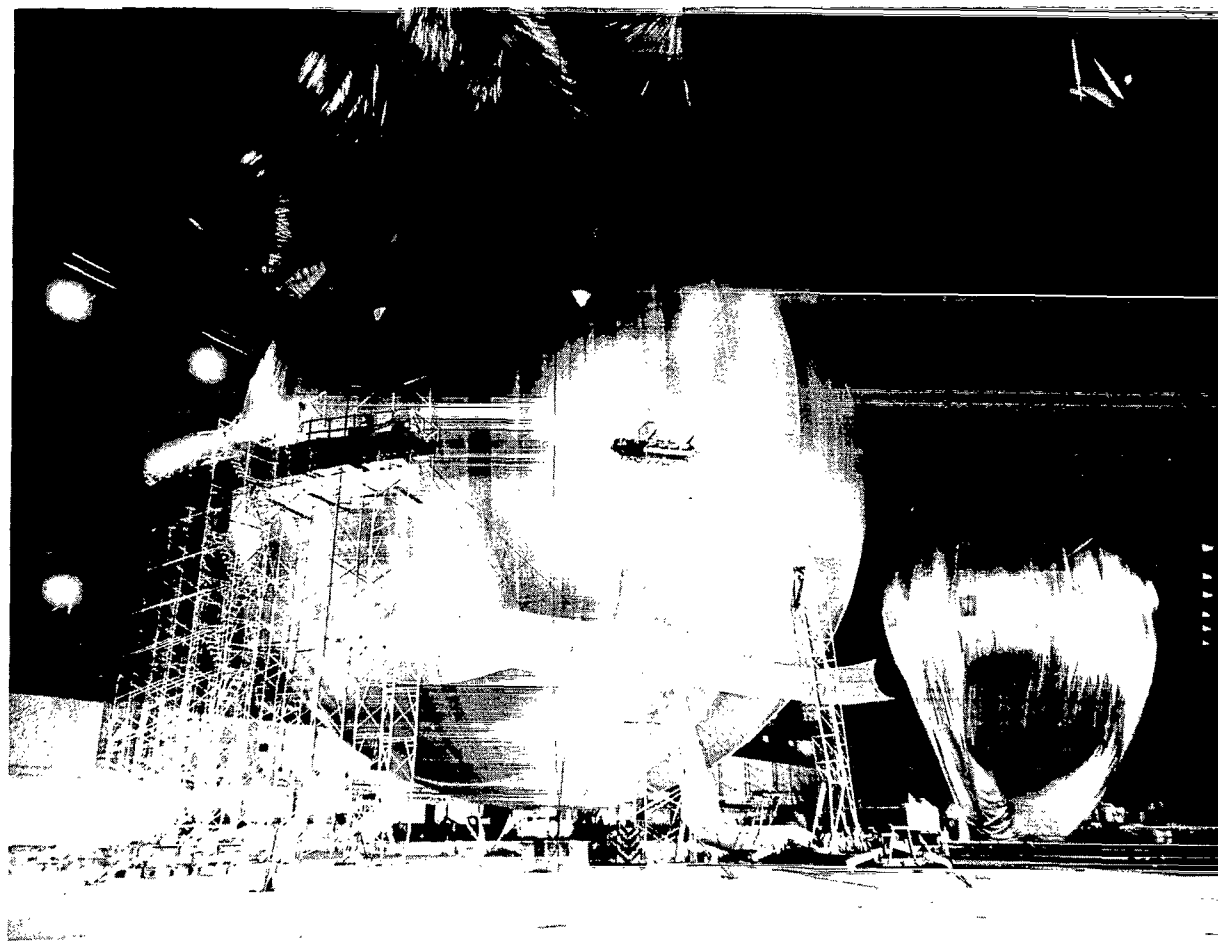

Figure 1—An overall view of the test setup employed for the Static Inflation Test.

and bottom of the balloon, were provided so that ambient air could be circulated within the balloon. This allowed for the dumping of cold air (bottom) and warm air (top) to obtain the required buoyancy. Pressure in the balloon was maintained at any desired level with automatically controlled dampers on the inlet and exhaust ports which regulated the amount of ambient air that was fed to the balloon. While this field test was not the first inflation experiment to be conducted,* it does herald the first attempt at evaluating a tethered balloon structure approximately thirteen stories high designed intentionally to remain fully suspended during the entire course of the test. Thus, this experiment afforded an opportunity of investigating the strain behavior of the metal-polymer film as it is subjected to increasing levels of biaxial stressing under programmed inflation schedules involving both pressurization and relaxation of the balloon envelope. An overall view of the test setup is shown in Figure 1.

The ultra-thin gauge of the Echo II laminate precluded determining strain behavior by such proven methods as mechanical or electric extensometers, electrical strain gauges, or even transparent photo-elastic coatings, because each suffers from one serious deficiency, i.e., each device necessarily introduces a reinforcement component (stiffness factor) that cannot readily be separated from the actual strain response of the laminate material by any presently acceptable calibration technique. For this reason, a very simple but direct measuring approach was proposed and subsequently implemented. It involved the measurement of change in strain developed by an expanding grid pattern (painted on the surface), with incremental increases in pressure.

The type of grid pattern used in the June-July tests on balloons 9, 11, and 13 is shown in Figures 2 and 3. The grid pattern was inked on the balloon skin and a paper frame was constructed to surround the grid. The necessary reference was established by coupling the frame to the balloon surface with rubber bands thus insuring that the frame dimensions would not change as the balloon expanded. The known distances between the four large dots located at the corners of the frame were then used as level points.

Using India ink, nine square grid patterns were applied to the surface of the balloon located approximately 10 degrees below the equator. Each 18×18 inch grid pattern consisted of 3/16 inch wide lines spaced 1 inch apart. Since the aim of this study was to investigate the strain distributions within individual gores and at the seams, the nine grid patterns were alternately placed to coincide with these regions of interest (Figure 4). These particular sections of the balloon surface were intentionally selected because they also represented the areas chosen for performing the stereo-photogrammetric experiments. Stereo mapping (Reference 1) of the balloon surface constituted one of the prime experiments of the static inflation tests from which profile and contour models of the envelope were developed as a function of biaxial stressing.

Photographs from two RC-8 Wild precision aerial cameras,† provided by the Army Map Service, were employed in registering whatever dimensional change occurred in the grid pattern

*Weeksville Test of Echo II conducted at Weeksville Naval Air Station, Elizabeth City, North Carolina, May 1961.
†Modified to a finite focal distance of 12.9 feet.

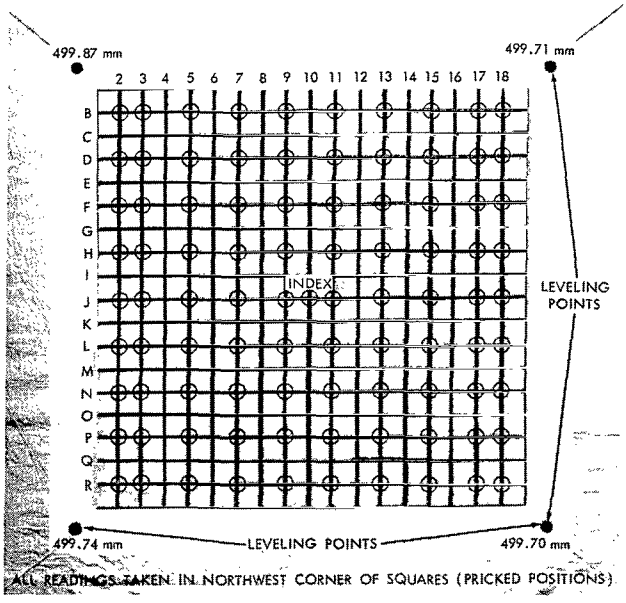

Figure 2—Photograph of the grid pattern used for photogrammetric strain analysis (Balloon 13 - July Tests). Picture taken at a skin stress level of 1500 psi. Note wrinkling in the skin.

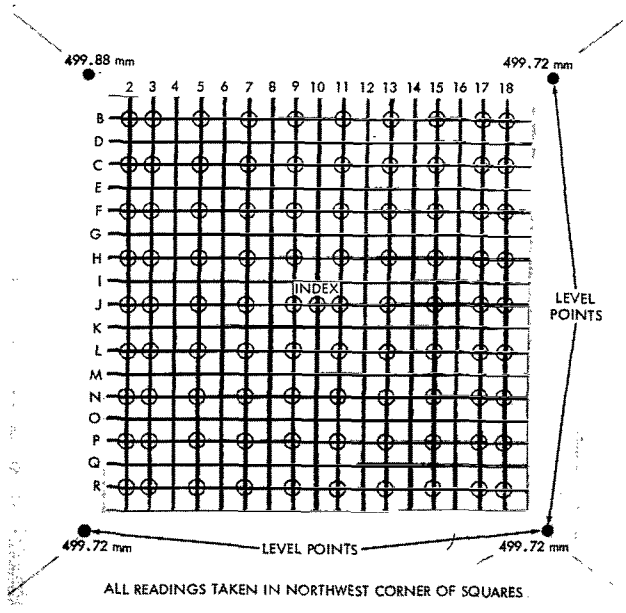

Figure 3—Photograph of the type of grid pattern used for the initial photogrammetric strain analysis (Balloon 13 - July Tests). Picture taken at a skin stress level of 7400 psi. Note smoother appearance of skin as compared to Figure 2.

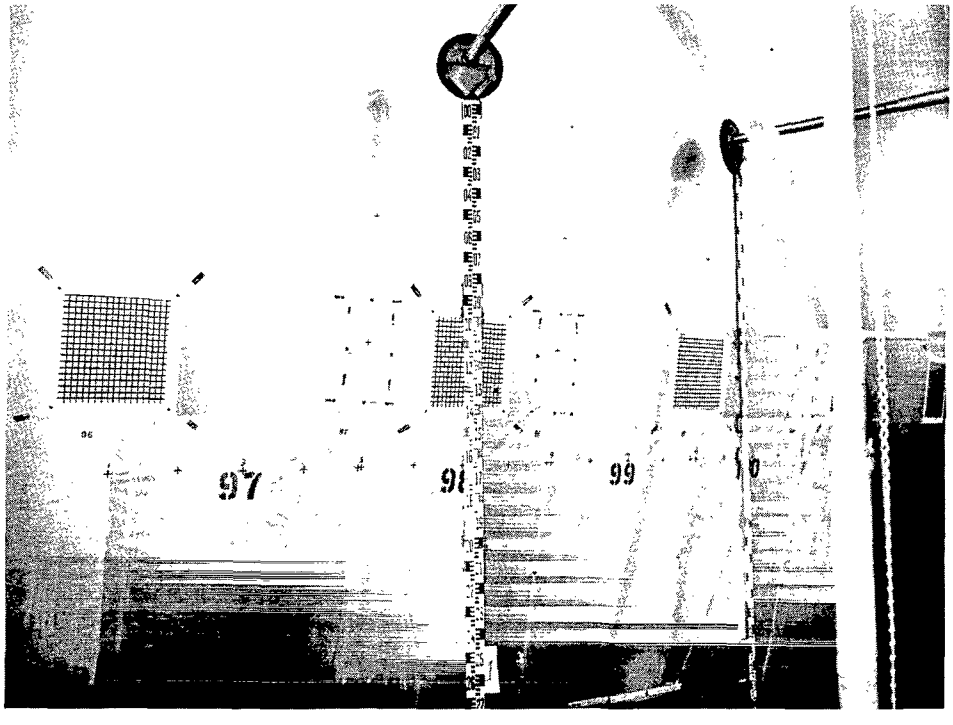

Figure 4—Photograph of portion of balloon showing location of grid pattern (July 1963 Tests). Typical for balloons 9, 11 and 13.

during the pressurization and relaxation schedules. The resulting strain measurements were then compared to the static-reference system that was constantly in the field of view of the cameras. For this initial attempt at evaluating the effect of internal pressure or skin distortion, two pressure levels corresponding to nominal stresses of 1500 and 2400 psi were analyzed. Coordinate listings of selected grid intersections were tabulated by using photogrammetric techniques. The results of this initial sampling of data were disappointing however, in that several problems not originally anticipated were revealed. It will suffice to say, at this time, that both inadequate pattern size and grid line variability were two prime factors responsible for precluding a quantitative evaluation of the skin behavior.

Based on this knowledge, an improved method for precise application of a target on the balloon surface was devised and subsequently implemented during the December prelaunch static inflation test on balloon 16. This change in technique, incorporating a precision dot pattern (Figures 5 and 6), made possible a more accurate measurement of dimensional changes.

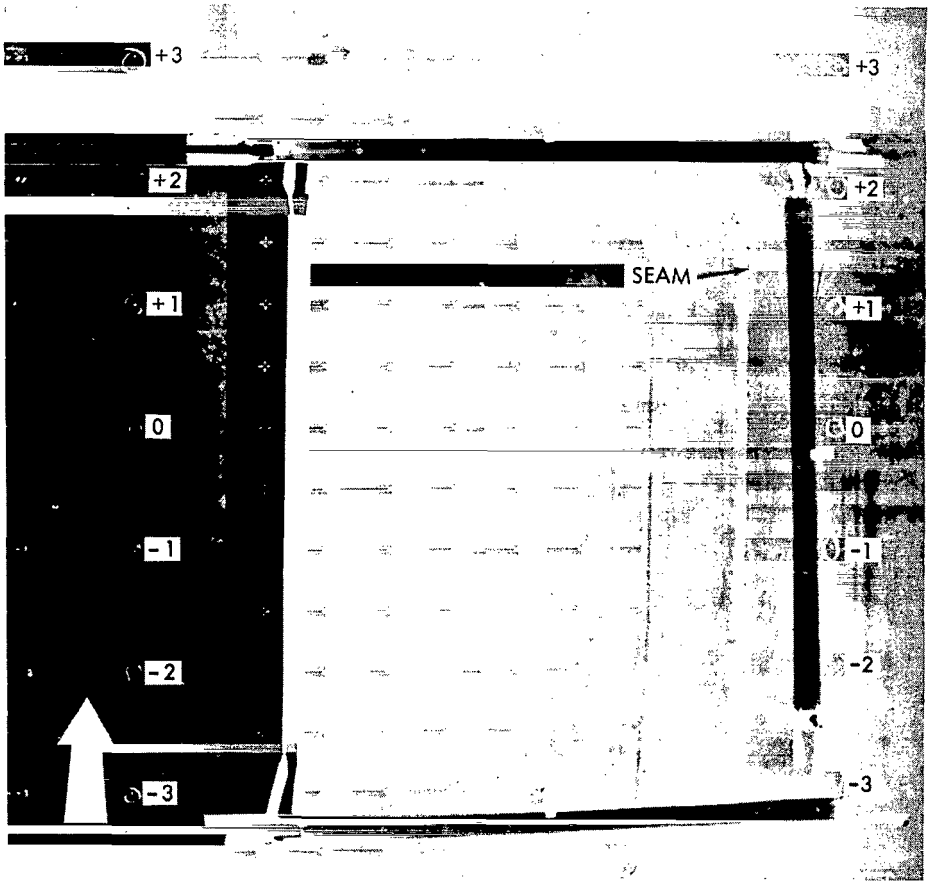

Figure 5—Photograph of grid pattern used on balloon 16 (December Test). Note "washing out" of some points due to poor lighting conditions. Pressure level approximately 20,000 psi.

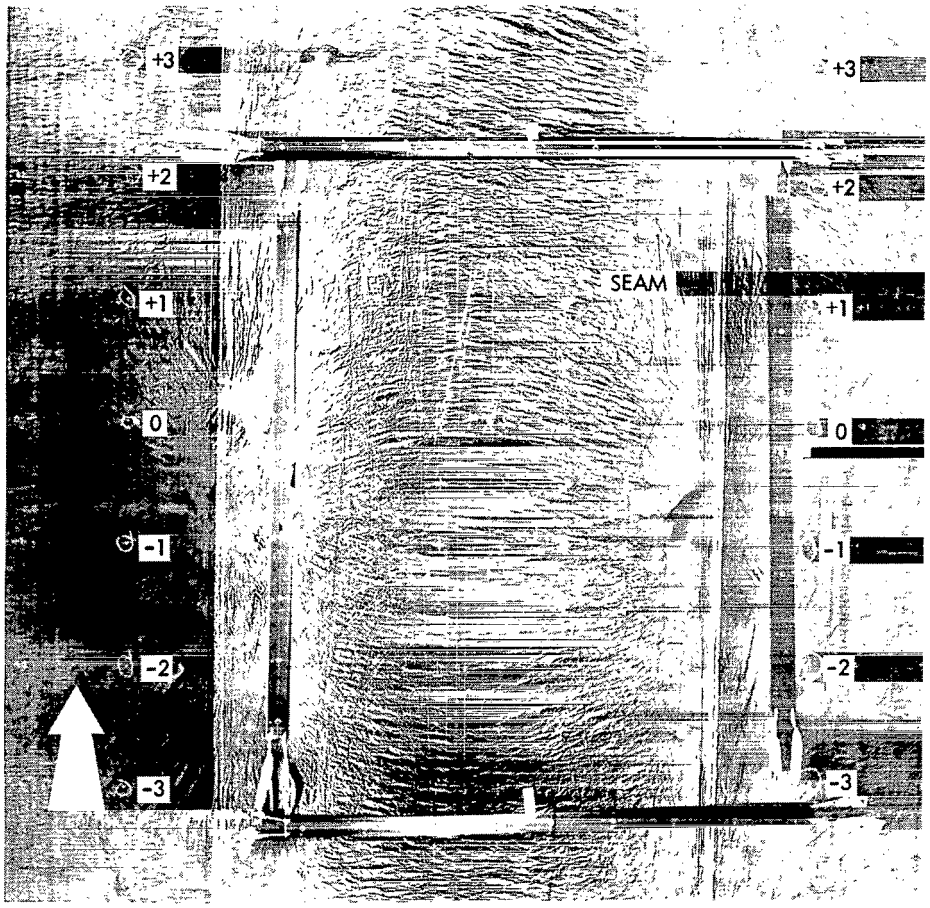

Figure 6—Photograph of grid pattern used on balloon 16. Note excessive wrinkling which obscured many points. Pressure level 1600 psi.

A dot grid pattern used on balloon 16 was applied to the "skin" material (X-15-2) during fabrication of the balloon, using a 2×8 foot precision template (10 mil polyester sheet) and Petikon type T plastic ink. The completed pattern covering an 8×8 foot section of the balloon consisted of 289 dots, each 1/16 inch in diameter and located 6 inches apart. The resulting eight foot square target was sufficient to cover gore number 5 (4 feet wide), and half of each adjacent gore 4 and 6. To permit recording of the pattern's displacement from a given reference scale and to correct for balloon tilt that may have developed during the test, four measuring bars with marks 6 inches apart and 4 feet long were made and attached to the balloon surface with rubber bands as shown in Figure 5. As the balloon expanded, the rubber bands stretched without developing any significant dimensional change in the tapes and permitted constant reference marks to be seen in each photograph.

The target was precisely placed on the selected gores at the contractor's facility (Reference 2) prior to their being seamed into a spherical balloon. However, when the balloon was shipped to the Lakehurst test site, it was discovered that the two gores adjoining gore 5 had been inadvertently

seamed in the wrong sequence, thus resulting in a disconnected dot pattern outside central gore 5. To rectify this mistake, it was decided to bridge the gap with 12 inch intervals using a cherry picker capable of spanning 70 feet as an elevated platform. Since the balloon, at the time, was very active and the target points were placed on the surface with difficulty, some error in alignment of the dot pattern was inevitable. In view of this fabrication error, an analysis of the accuracy to be ascribed to the target placement was made and is defined as follows:

1. The points on the central gore 5 are accurate to ±0.001 inch;
2. The points on the four control bars are accurate to ±0.001 inch;
3. The points on the adjacent gore halves are not considered accurate.

It is estimated that these fiducial points are in no better than a ±0.25 inch relation to each other and in a ±0.50 inch relation to points across the gore seam. The grid was photographed at successive stages of inflation using an RC-8 Wild camera and Kodak Double-X Ester Base Aerographic film. From these photographs, the Army Map service was able to reduce the grid pattern to an X-Y coordinate system listing tables of grid intersection points for each of twelve inflation pressure levels.

TEST RESULTS

The following is a description of the data reduction and analysis of the photogrammetric strain measurements obtained during the June and December static inflation experiments.

June-July Static Inflation Test

The coordinate system for the grid pattern representing the June tests is explained as follows:

Rows were lettered B through R and columns marked 2 through 18, (Figure 2). With the stereo comparator, distances from a given reference index designated (J-10) were determined for each coordinate point. Thus, the distance between any two horizontal or vertical points on the grid could be obtained by simple subtraction of the tabulated coordinate point. An analysis of the magnitudes and distribution of strain exhibited by the grid target located in the center of gore 98 of balloon 13 at two substantially different pressure levels (1500 psi and 7400 psi) was performed. The surface appearance at these pressure levels is shown in Figures 2 and 3 respectively. For our purpose, a sampling of 10 grid intersections, equally distributed between horizontal and vertical directions was selected for analyses. The results are reported in Table 1 and represent the magnitude of observed grid distortions in terms of linear strain (ϵ) which is simply the change in length ($\Delta\ell$) in a given direction divided by the original length (ℓ_o) of this grid spacing expressed in percent. Thus

$$\%\epsilon = \frac{\Delta\ell}{\ell_o} \times 100 \ . \tag{1}$$

Table 1

Static Inflation Test
Strain Measurements Balloon 13 (1500 psi - 7400 psi).

Strain Direction	Grid Line	Coordinate (1500 psi)	Coordinate (7400 psi)	Strain (percent)*
Horizontal	B2-B18	33.01	33.14	0.39
Horizontal	D2-D18	33.04	33.17	0.39
Horizontal	H2-H18	33.01	33.17	0.48
Horizontal	L2-L18	33.19	33.30	0.33
Horizontal	P2-P18	33.20	33.32	0.36
				Average 0.40
Vertical	B2-R2	32.90	33.05	0.46
Vertical	B5-R5	32.90	33.10	0.61
Vertical	B9-R9	32.94	33.12	0.49
Vertical	B15-R15	32.02	33.18	0.50
Vertical	B18-R18	32.98	33.09	0.33
				Average 0.48

$$*\text{Strain} = \frac{\text{Coordinate at 7400} - \text{Coordinate at 1500}}{\text{Coordinate at 1500}} \times 100.$$

These results indicate a significant variation in total strain for the pressure levels selected with a maximum value of approximately 0.61 percent developed in the vertical direction. Comparison of their respective means also shows that the magnitudes of strain in the vertical direction are significantly more than those observed in the horizontal direction. This bias may be explained by the unbalanced forces resulting from the component of lift acting on the upper sections of the balloon and the counter force due to gravity which is added to the uniform force due to pressure.

The degree of deviation from the mean observed in both directions is an indication of the non-uniform distribution of strain developed by the envelope. However, because of the relatively small size of the grid and the variable width of the grid lines, it was difficult to ascertain precisely the points selected for measurement by means of the stereo comparator. As a result, the coordinate values obtained reflect an error of measurement that cannot easily be separated quantitatively from the actual strain response of the skin material, and therefore, a portion of the erratic strain results must be assigned to dimensional inaccuracy associated with the grid patterns. Obviously, a more precise grid pattern was necessary before confident results could be obtained and so, an improved target pattern was developed for balloon 16 which was scheduled for testing in December 1963.

December Static Inflation Test

An effort was made to study the strain behavior at every point on the improved grid pattern at each increment of pressure. It was expected that such an experiment involving this rather complex composite film could provide the information needed to determine the state of stress and strain obtained at the sites selected for study. However, because of rather poor lighting conditions in which there was either an excess of light reflecting from the smooth surface of the balloon at the higher pressure levels (Figure 5) resulting in certain points on the pattern being "washed out" or a defficiency of light in which the points were too dark and obscured by the wrinkled texture of the balloon skin (Figure 6), results of this study were not as fruitful as anticipated. In comparing the resulting strain-pressure relationships, it was noted that in a few instances, an incremental pressure rise did not produce the expected increase in strain. On the contrary, either no change was registered or more surprising, a decrease was observed. This anomaly, however, is attributed to the fluctuating pressure obtained in the balloon and to the irregularities in the skin evident at the lower inflation pressure levels. Therefore, the range of pressure over which linear strain was to be measured was expanded to cover from 0.028 inH_2O to 0.124 inH_2O and from 0.028 inH_2O to 0.500 inH_2O. The former applies essentially to the elastic portions of the stress-strain curve for aluminum while the latter reflects the behavior of the oriented polymer close to its ultimate strength. The lowest pressure level (0.018 inH_2O) obtained at the start of the test was not used in the analysis because the existence of excessive wrinkles in the skin precluded accurate measurements of strain response. For the pressure ranges (0.028 - 0.124 and 0.028 - 0.500 inH_2O) an analysis of the strain pattern was made along and across each seam observed in the dot pattern, as well as within the gore area. The previously mentioned targets (Figures 5 and 6) were purposefully located on the balloon so as to overlap two seams and to extend above and below the equatorial region of the balloon.

Figure 7 is a schematic representation of the grid patterns shown in Figures 5 and 6 together with the calculated strain shown between the various points. The four rectangles represent the standard tapes which did not change dimensions with pressure. The points on these tapes were separated by known distances and could, therefore, be used to compute absolute distances on the balloon from the photographs, if so desired.

The individual points are identified by a coordinate system designated by rows numbered 5, 7, 9, 11, 13, and 15 and by columns numbered 10a, 10b, 3a, 2a, 4, 6, 8. This numbering system applied when north was at the top of Figure 7.

Average strains are presented in Table 2 in which the values represent individual strain measurements from points above and below the equator. Similar averages were taken along each seam and across each seam both north and south of the equator as well as within the gore itself.

The strain results, summarized in Table 2, also illustrate the degree of non-uniformity in skin distortions exhibited by the balloon material for two different levels of inflation pressure. In general, it appears that the upper half of the balloon (north of the equator) develops significantly more plastic deformations than do corresponding regions of the lower half. For example, the

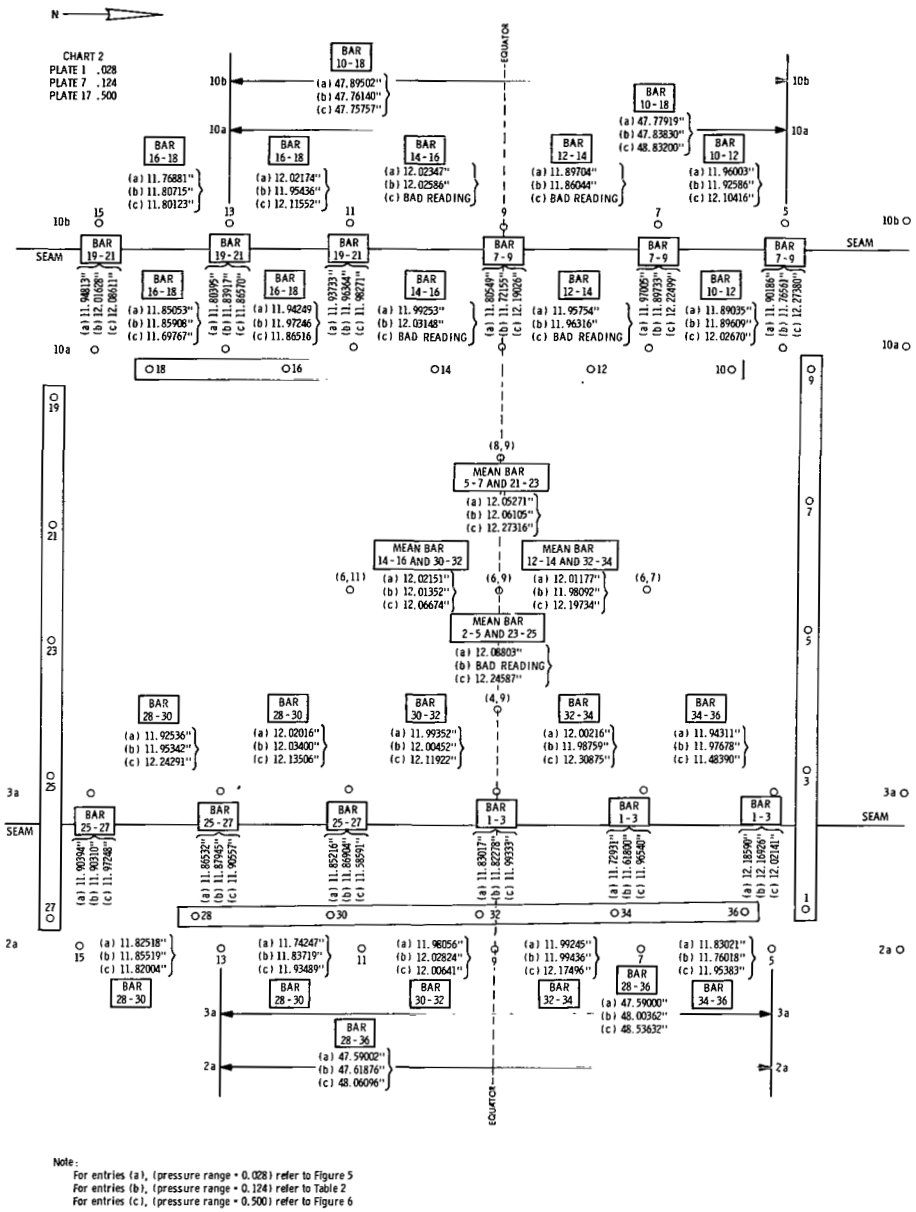

Figure 7—Schematic representation of grid pattern shown in Figure 5 showing calculated strain values.

magnitude of strain developed across individual seams located north of the equator is approximately 3 to 4 times greater than the values measured across the same seams located below the equator. A similar pattern was noted for the strains measured in a direction parallel to the seams, though to a lesser extent. This asymmetrical strain behavior is attributed in part to the dead weight loading associated with the lower portion of the balloon and to the inherent differential air density existing within the structure, both of which directly affect the configuration assumed by the

Table 2

Strain Measurements Obtained by Photographic Techniques.

Position of Measurement	Average Strain (percent)* Pressure Range (inH_2O)	
	0.028-0.124	0.028-0.500
Across West seam North of Equator	No data	2.8
Across West seam South of Equator	0.363	0.69
Across East seam North of Equator	No data	1.67
Across East seam South of Equator	0.130	0.46
Along West side of West seam - North of Equator	No data	1.21
Along West side of West seam - South of Equator	0.173	0.53
Along West side of West seam - North to South	0.173	1.8
Along East side of West seam - North of Equator	0.0477	1.15
Along East side of West seam - South of Equator	0.216	No data
Along East side of West seam - North to South	0.149	2.2
Along West side of East seam - North of Equator	0.282	1.45
Along West side of East seam - South of Equator	0.147	1.56
Along West side of seam - North to South	0.181	1.99
Along East side of East seam - North of Equator	0.0159	1.28
Along East side of East seam - South of Equator	0.486	0.93
Along East side of East seam - North to South	0.492	0.99
Center of gore East-West	0.0692	1.69
Center of gore North-South	No data	0.96

*Values are average of two and sometimes three values depending on the particular points involved. In some instances, there is only one value available.

envelope. The results of the earlier photogrammetric studies (Reference 3) carried out concurrently on the balloon, are consistent with the pattern of strain revealed by the grid experiment. Specifically, the contour charts indicate that the balloon continuously assumed an oval shape (vertical dimension greater than equatorial dimension) even at the highest levels of *skin* stress studied. The average percent strain developed along both test seams was 1.16 percent while that observed in the transverse directions, across the same seams, was 1.77 percent. The magnitudes of the difference appear significant; however, as mentioned earlier, the target points of both adjacent gores can be considerably in error. For this reason, only a qualified trend is at best suggested by the data. Strains of 1.69 percent in the east-west direction and 0.96 percent in the north-south direction across the gore at the equator (Table 2) corroborate these results. For the pressure range 0.028-0.124 inH_2O, the comparison between strain values *across* the seams north and south of the equator is not possible, due to the fact that data from some of these points are missing. However, the most significant fact obtained from the strain values for this pressure range is that

when the average of all the strain measurements *along* both seams north and south of the equator, 0.215 percent, is compared with the average of all the strain values *across* the seams both north and south of the equator, 0.243 percent, the difference is not as great as were the same measurements for the pressure range 0.028-0.500 inH_2O, indicating in this case some degree of balanced biaxiality. This is reasonable because the elastic limit has not been exceeded at this pressure whereas at 0.500 inH_2O the elastic limit has been exceeded and a deviation from balanced biaxiality can be expected.

A comprehensive membrane analysis (Reference 4) involving an idealized pressurized spheroid was performed by Hossein Bahiman in which, for this theoretical treatment, it was assumed that displacement due to gravitational forces was negligible and that the envelope consisted of a material that was homogeneous, isotropic and linearly elastic. By choosing suitable elastic constants, a calculation of the amount of strain produced by a given pressure level is obtained when the solution derived from the preceding analysis is employed. Such a computation was carried out for a series of inflation pressures and the resulting strains are presented in Tables 3 and 4 together with a sample calculation which is included in Appendix A. Table 4 also includes values of strains obtained experimentally for the corresponding pressure ranges. The marked discrepancy between theory and experiment for the 0.028-0.084 inH_2O and 0.028-0.500 inH_2O pressure ranges is not surprising and can be explained in the following manner. At the lowest pressure level, grid distortion is due primarily to the inherent initial unwrinkling of *skin* creases and other surface flaws, and therefore, the assumption that the strain response of the balloon envelope is directly proportional to inflation pressure is not valid. On the other hand, it is obvious that when the level of pressure is increased to the point where the material departs completely from elastic behavior, the calculated quantity is rendered meaningless. However, to indicate the possible error which can be introduced when plastic deformation prevails, the theoretical calculation was included in Table 4. The agreement between theory and experiment is much better when the intermediate pressure ranges 0.028-0.110 and 0.028-0.124 inH_2O are compared. This is predictable since both pressure levels result in nominal skin stresses that probably still represent the elastic plastic range of the material. The ratio of experimental to theoretical strain corresponding to these pressure ranges is 0.563 and 0.564 respectively. In view of the complex patterns of strain

Table 3

Strains Obtained from Theoretical Calculations.

Differential Pressure (inH_2O)	Skin Stress (psi)	Theoretical Strain (percent)
0.028	1,120	0.183
0.084	3,360	0.252
0.110	4,400	0.301
0.124	4,560	0.314
0.500	20,000	0.930

Table 4

Comparisons of Theoretical Measured Values of Strain.

Pressure Range (inH_2O)	Strain* (percent)	
	Experimental	Theoretical
0.028 - 0.084	0.379	0.069
0.028 - 0.110	0.0664	0.118
0.028 - 0.124	0.0692	0.123
0.028 - 0.500	1.69	0.747

*Strain within the Gore - East-West Direction.

revealed by the photographic data and the attendant errors associated with the assumptions employed in the analysis (estimated to be approximately 30 percent), the observed deviation is considered reasonable.

In order to ascertain the quality of the balloon material used in fabricating the static inflation test balloons, a limited program involving tensile and bulge tests was carried out and these results are summarized in Tables 5 and 6. In addition, the rupture strengths of the balloons tested in both June-July and December, 1963 are presented in Table 7. These data are presented in an attempt to show some correlation between laboratory tests and photographic measurements made in the field.

Table 5

Tensile Test.

Material*	Yield Strength (0.2 percent offset) (psi)	Tensile Strength (psi)	Elongation (percent)
Room Temperature Roll-Longitudinal	10,480	23,720	5.2
Room Temperature Gore Material (X-15-2) - Longitudinal	11,772	25,182	11.5
Room Temperature Gore Material (X-15-2) - Transverse Direction	10,795	23,545	15.16
Room Temperature Mylar	9,923	18,125	42.0

*Head speed 0.05 in/min except mylar which was run with head speed of 0.02 in/min.

Table 6

Bulge Test.

Material	Pressure (mmHg)
Room Temperature Roll	114.5
32°F Roll	153.4
Mylar Room Temperature	93.4
Mylar 32°F	108

Table 7

Balloon Results.

Balloon	Test	Material	Pressure (inH_2O)	Rupture Strength (psi)
9*	June	X-15	0.105	4,200
11	June	X-15	0.158	6,200
13**	July	X-15	0.28	11,200
16	December	X-15-2	0.58	23,200

*This balloon failed at the base exhaust port and was considered a structural rather than a material failure.

**This balloon failed at the lower exhaust duct and also was not considered a material failure.

Tensile Tests

The tensile tests were performed on sample laminate material taken at random during the lamination improvement program. This material was designated as "roll" material. Similar tests were performed on laminate material, designated X-15-2, intended for use in balloon 16 (the December test balloon). The X-15-2 material differed from roll material in that certain variables in the lamination process were changed which resulted in a stronger, more defect-free material (see page 14). The material was tested in both the longitudinal and transverse directions with the specimen axis respectively parallel and perpendicular to the original rolling direction.

A comparison of the tensile properties of the roll and X-15-2 material tested in the longitudinal direction showed not only a higher yield and tensile strength in the X-15-2 material but also a remarkable increase in elongation. Comparison of the X-15-2 material tested in the transverse and longitudinal direction disclosed slightly lower tensile and yield properties and higher elongation in the transverse direction. An examination of the tensile properties of the mylar as compared to the laminate indicated a higher tensile strength and yield and lower elongation of the laminate material which were attributed to the reinforcing effect due to the addition of two layers of aluminum foil to form the laminate structure.

Biaxial Bulge Tests

Concurrent with the static inflation test experiment, a lengthy series of biaxial bulge tests was performed in order to duplicate more nearly the type of stressing the balloon would see in service.

For this purpose, a device was designed and constructed to permit balanced biaxial stressing of an 11 inch diameter diaphragm. By employing a vacuum, the sub-size specimen was subjected to a uniform pressure distribution on its surface (the atmosphere). Figure 8 shows the equipment used for this study. During the test, a continuous measurement of chamber pressure was recorded in which the differences between the initial pressure in the chamber (atmospheric) and the final pressure recorded corresponded to the burst pressure. The state of stress corresponding to each pressure level could be determined if so desired. However, since pressure is related to stress and our interest was solely directed toward determining relative levels of strength, this operation was not carried out. Also shown in Figure 8 is a proximity device which automatically followed the surface of the specimen as it was deflected, and that movement was also continuously recorded since this deflection can be related to strain. These tests were intensified after the failures of balloons 9, 11, and 13 (Reference 3). A sampling program was devised in which the G. T. Schjeldahl Company supplied GSFC with samples from each roll of material together with the appropriate gore number for balloon 16 so that a quality control check on the material could be conducted. During the course of these studies, over 800 individual tests were run. It was noted that certain rolls were of good quality while others were questionable, and still others were completely unacceptable. During these tests it became apparent that the test of balloon 16 would be run at temperatures near the freezing point so, additional bulge tests were run on roll material and mylar at 32 degrees F in order to determine the change in properties due to the lower temperature. Results of these tests are tabulated in Table 6. As anticipated, at the lower temperatures the laminate material increased in bulge strength by approximately 34 percent over room temperature tests and the mylar increased by approximately 16 percent. Using these data and accepting the theoretical strength of the balloon as approximately 9,000-13,000 psi,* we anticipated that balloon 16 could theoretically reach a skin stress of from 9,270 to 23,400 psi. Examination of Table 7 shows the results of the tests on the balloon and a burst strength of 23,200 psi for balloon 16.

*This value has been in question since the start of the project and has not been sufficiently determined even at this time.

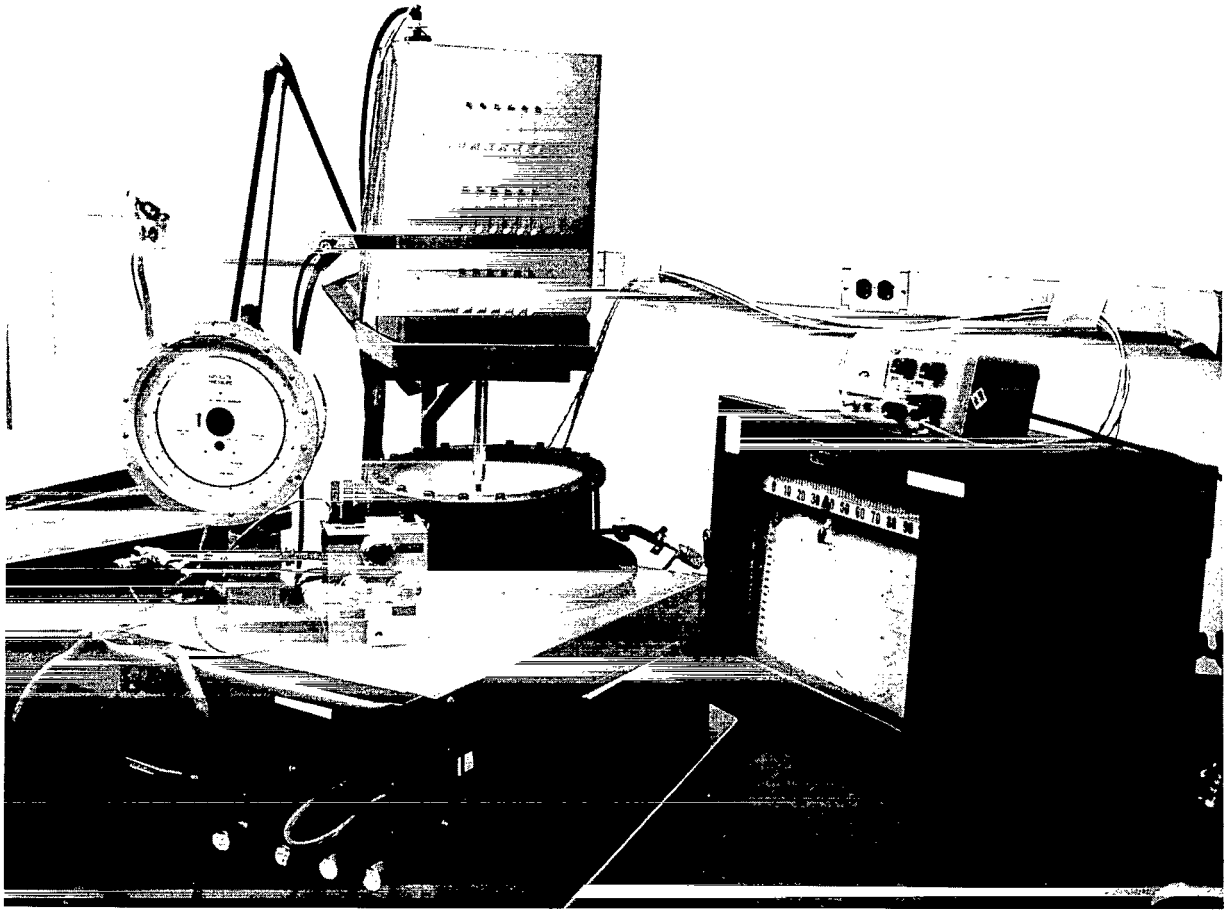

Figure 8—Photograph of bulge test setup.

DISCUSSION

Analysis of strains calculated from photogrammetric data of the first grid pattern experiments (June tests) indicated considerable variation in the strain between specific points. The average strain of horizontal and vertical components did, however, show some degree of balanced biaxiality with slightly more strain occurring in the vertical than in the horizontal direction. This was not surprising since the greater strain would result from additional vertical forces developed due to lift and the reaction of gravity. However, because of the crudeness of the grid pattern, it was decided to improve its design for the December tests in the hope that more precise data could be obtained with the new pattern.

Analysis of the strain behavior in balloon 16 by the photogrammetric technique in December was not as fruitful as had been originally anticipated, especially in the quantitative analysis of specified points at each increment of pressure. This technique, however, proved very useful in

determining the overall distribution of the strain pattern on the balloon in the area of the grid pattern. For the pressure range 0.028-0.500 inH_2O it was observed that in general, the strains north of the equator were higher than the strains for points located at similar distances below the equator. In addition, grid pattern distortion observed within the gore indicated a non-uniform state of strain did exist in the envelope. The average strains measured *along* and *across* both seams were 1.16 and 1.77 percent respectively which is a significant difference. These results, however, were not surprising for this pressure range because it exceeded the elastic range of the material and, therefore, biaxiality would not be expected. The non-uniformity of the strain patterns north and south of the equator was probably due to various factors including the lifting effect of the balloon due to the warm air in the balloon, together with the counter action of gravity. Other properties including reinforced gores, instability due to atmospheric conditions, and the inclusion of intake and exhaust ports in the balloon all lead to the complexity of the strain patterns observed. Within the elastic range of the material, corresponding to a pressure range of 0.028-0.124 inH_2O, the strains observed were more balanced. The average strain measured *along* both seams north and south of the equator was 0.215 percent, whereas the average strain measured *across* both seams north and south of the equator was 0.243 percent. The difference was not great, which indicates considerable biaxiality was present in the material for this pressure range.

Comparison of the experimental values of strain with those calculated for the intermediate pressure range revealed a significant discrepancy. This difference, however, which is attributed to the numerous assumptions used for developing the theoretical equations and the complexity of strains shown to exist by the photographic examinations of the grid patterns, is considered to be within reasonable limits.

Supplemental information involving tensile and bulge tests data, provides more specific information with regard to the strength properties of the laminate material. After the premature failures of balloons 9 and 11 and the uncertainty in the values connected with balloon 13, an investigation was undertaken to determine the cause of these failures. Examination of the gores in the vicinity of the fracture revealed the presence of a particular recurring surface flaw induced in the film during the laminating process. These flaws, acting as stress raisers, were sites from which the initial crack started and along which the crack propagated.

These defects were subsequently eliminated by incorporating the following changes in the laminating process:

1. Reduction of the curing temperature using to set the adhesive bond in the film.
2. Reduction of the speed of the laminating process.
3. Reduction of laminating film width from 54 to 24 inches which improved tension control of the film during fabrication.

As a result, samples of this improved material (designated X-15-2 material) were sent to GSFC for testing. Additional samples of X-15-2 material tested in the longitudinal direction showed a

higher yield strength and tensile strength for the X-15-2 material. When X-15-2 material was tested in the transverse direction, a noticeable lowering in strength properties was observed as compared with the same material tested in the longitudinal direction. This weakness in the transverse direction was exemplified by bulge tests in which the material generally failed in the transverse direction. Balloons 9 and 11 also showed evidence of an initial transverse crack, (Figure 9). Tensile tests of the mylar showed a tensile strength of 18,000 psi. When fabricated into the laminate material, the laminate tensile strength increased to 24,200 psi in the longitudinal direction. Since the aluminum foil has a relatively low tensile strength (6,800 psi in the annealed condition) it is obvious that the mylar at the higher loads is providing the bulk of the strength of the laminate. The tensile strength exhibited by the composite (25,200 psi) therefore, must be due to another factor which is probably the adhesive.

Since it was known that the December test would be carried out at temperatures near freezing, an investigation of the properties of the laminate and mylar was carried out in the bulge test

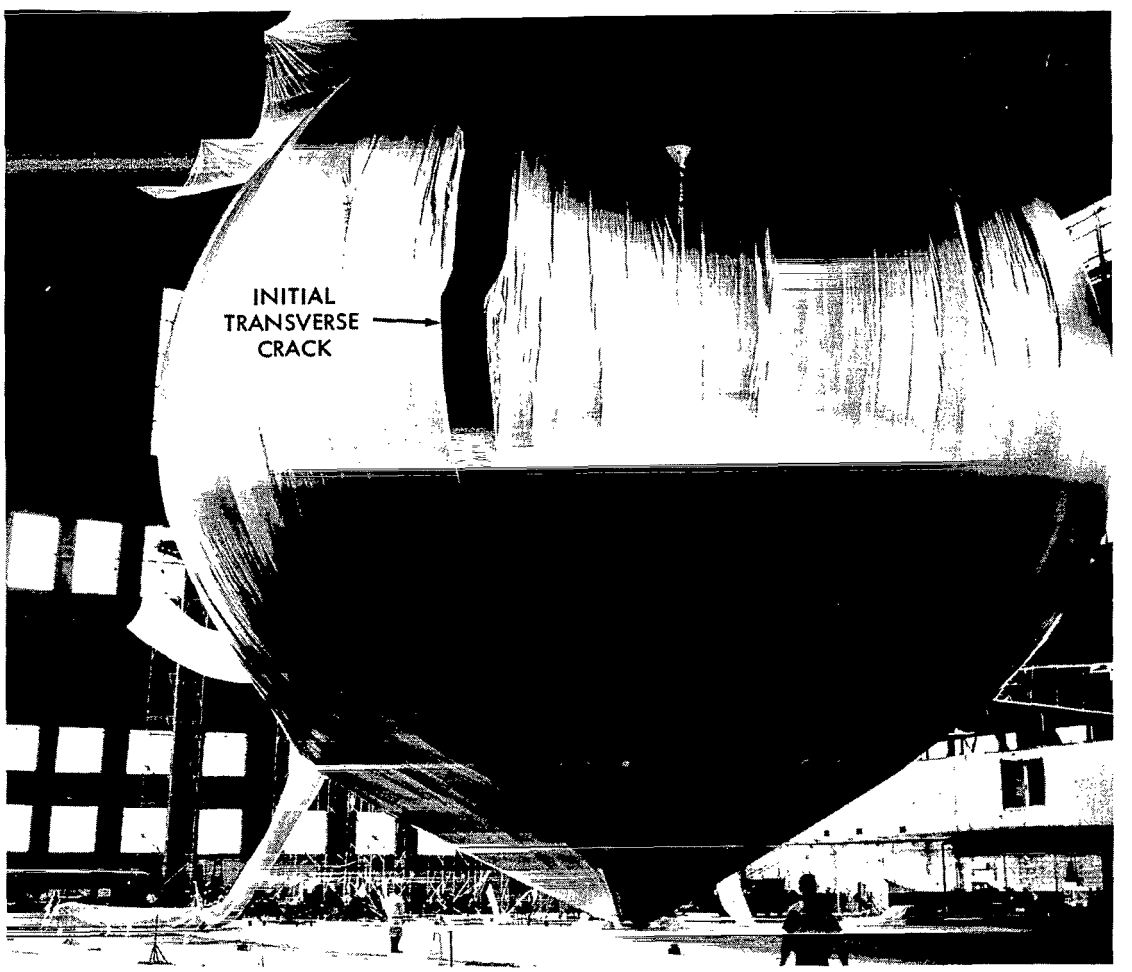

Figure 9—Photograph of failure area in balloon 11 (June Test) showing evidence of an initial transverse crack.

apparatus at room temperature and at 32 degrees F. As anticipated, an increase in the bulge strength of the laminate was observed. This increase was approximately 34 percent. The increase in the bulge strength of the mylar, however, was only 16 percent at 32 degrees F. The increase in bulge strength of the laminate over the pure mylar is not attributed to the aluminum, which starts to crack at relatively low bulge pressures, but must again be attributed to the adhesive. Based on these low temperature studies, however, and knowing an approximate theoretical burst strength of the balloon (maximum of 18,000 psi) it was possible to estimate that balloon 16 could increase its skin stress by approximately 34 percent yielding an ultimate skin stress of 23,400 psi maximum. Results shown in Table 7 revealed the agreement between the field test and the calculated values.

CONCLUSIONS

The photogrammetric technique for measuring the strain patterns on the test balloons has been demonstrated, and can be used for similar work on future projects. Improvements incorporating stereographic techniques and synchronization of the photographs with an exact pressure measurement would eliminate discrepancies such as occurred where observed distances decreased with an apparent increase in pressure. The photogrammetric measurements, while not fulfilling all the anticipated requirements did provide a reasonable picture of the complex strain pattern set up in the balloon during the static inflation tests.

There is apparently, no rigorous way of correlating the photogrammetric technique with the tensile and bulge test data in this series of tests. However, there is considerable correlation between tensile and bulge test data and actual balloon conditions. It is also apparent that the properties of the laminate adhesive material are more important than had been realized to date.

ACKNOWLEDGMENTS

The authors wish to acknowledge the help of the Army Map Service which provided the technicians needed to obtain the photogrammetric measurements at the static inflation test site. Special thanks is given to Mr. Richard Underwood of that agency whose help in all phases of the program is greatly appreciated. Acknowledgment is also extended to Dr. Hossein Bahiman of the GSFC, for the use of his theoretical calculations, and to Dr. Bahiman and H. Horiuchi for their thorough review of this paper.

(Manuscript received July 22, 1965)

REFERENCES

1. Genatt, S., "Stereo-Photography of the Echo II Balloons Numbers 9, 11 and 13," GSFC Document X-524-63-259, December 17, 1963.

2. "Final Report on Contract NAS 1-1138," March, 1964 by G. T. Schjeldahl Co., Northfield, Minnesota.

3. "Final Report Echo II Static Inflation Test Number 2," November 1, 1963, GSFC.

4. Bahiman, H., "Membrane Analysis of Pressurized Thin Spheroid Shells Composed of Flat Gores, and Its Application for Echo II," NASA Technical Note D-3002, October, 1965.

Appendix A

The Use of Non-Linear Differential Equations in Obtaining Values for Strain at Various Pressure Levels

The calculations of the theoretical strains used in the paper were based on a series of five non-linear differential equations in terms of a_o, b_o, c_o, d_o, f_o, g_o, a, b, c, d, etc. developed by Dr. Hossein Bahiman of GSFC.* The initial solution lead to equations by which these coefficients can be evaluated.

To illustrate the use of these equations in obtaining a value for strain at any particular pressure level, consider the sample calculation

Assumed pressure level = 0.084 in H_2O,

0.084 inH_2O = 0.00304 psi internal pressure

Defining a parameter m, equal to $pr/k\alpha^2$ where p = internal pressure (psi) and k, α, and r as defined in the referenced publication;

$$m = \frac{pr}{k\alpha^2}$$

$$= \frac{0.00304 \times 810}{800 \times 0.00088}$$

$$= 3.50 \ . \qquad \text{(A1)}$$

Using the table of m versus B, developed by Dr. Bahiman, a value of B associated with m = 3.50 can be obtained. This will allow an evaluation of the coefficient d_0:

$$d_o = \frac{2B^2}{3} - \frac{\mu}{3} B \ , \qquad \text{(A2)}$$

where μ (Poissons ratio) = 0.33. Thus, by substitution of μ and B:

$$d_o = -0.0356 \ .$$

*NASA Technical Note D-3000.

Then

$$\gamma = \frac{1}{3} B^2 + \left(\frac{1}{2} + \frac{\mu}{3}\right) B$$

$$= -0.125 \ . \tag{A3}$$

By substituting the appropriate values of B, μ and γ, it is found that

$$F_1 = \frac{2\mu B + 1 + \mu^2}{-4\mu^2 B - 2\mu B + \mu^2 - 1} \ ,$$

$$F_1 = -1.15 \ . \tag{A4}$$

In a similar manner, values for A_1, A_2, C_1 and C_2 are found using the equations

$$A_1 = \frac{\mu\gamma + (2+\mu)}{2\mu B - \mu - 1} F_1 \ ,$$

$$A_1 = 2.02 \ ; \tag{A5}$$

$$A_2 = \frac{(\mu - 2B)\left(F_2 - \gamma\right) + \frac{pr}{k\alpha^2}}{1 + \mu - 4\mu B - 2B} \ ,$$

$$A_2 = 1.095 \ ; \tag{A6}$$

$$c_1 = \gamma + A_1 + F_1 = 0.745 \ ;$$

$$c_2 = A_2 - F_1 + \gamma \ , \tag{A7}$$

$$= 2.120 \ ;$$

(A8)

and

$$c = c_1 + c_2 \ . \tag{A9}$$

The strain is then

$$\epsilon\Big|_{\substack{x_0 \\ \theta=0}} = c\alpha^2 \ ,$$

$$= 0.252 \text{ percent} \ . \tag{A10}$$

To obtain values of strain for a particular pressure range shown in Table 4, the usual procedure followed is

$$\text{percent strain} = \frac{\epsilon_2 - \epsilon_1}{\epsilon_1}, \tag{A11}$$

where ϵ_2 is the strain of higher pressure levels and
ϵ_1 is the strain at lower pressure levels.

"The aeronautical and space activities of the United States shall be conducted so as to contribute . . . to the expansion of human knowledge of phenomena in the atmosphere and space. The Administration shall provide for the widest practicable and appropriate dissemination of information concerning its activities and the results thereof."

—NATIONAL AERONAUTICS AND SPACE ACT OF 1958

NASA SCIENTIFIC AND TECHNICAL PUBLICATIONS

TECHNICAL REPORTS: Scientific and technical information considered important, complete, and a lasting contribution to existing knowledge.

TECHNICAL NOTES: Information less broad in scope but nevertheless of importance as a contribution to existing knowledge.

TECHNICAL MEMORANDUMS: Information receiving limited distribution because of preliminary data, security classification, or other reasons.

CONTRACTOR REPORTS: Technical information generated in connection with a NASA contract or grant and released under NASA auspices.

TECHNICAL TRANSLATIONS: Information published in a foreign language considered to merit NASA distribution in English.

TECHNICAL REPRINTS: Information derived from NASA activities and initially published in the form of journal articles.

SPECIAL PUBLICATIONS: Information derived from or of value to NASA activities but not necessarily reporting the results of individual NASA-programmed scientific efforts. Publications include conference proceedings, monographs, data compilations, handbooks, sourcebooks, and special bibliographies.

Details on the availability of these publications may be obtained from:

SCIENTIFIC AND TECHNICAL INFORMATION DIVISION

NATIONAL AERONAUTICS AND SPACE ADMINISTRATION

Washington, D.C. 20546